Expanding foam as the material for fabrication, prototyping and experimental assessment of low cost soft robots with embedded sensing

Luca Somm, David Hahn, Nitish Kumar*, Stelian Coros

***Abstract*—Fabricating robots from soft materials imposes major constraints on the integration and compatibility of embedded sensing, transmission, and actuation systems. Various soft materials present different challenges, but also new opportunities, for novel fabrication techniques, integrated soft sensors, and embedded actuators. For instance, extensive research on silicone elastomers has led to the development of soft sensors based on closed channels filled with liquid metal conductors, as well as corresponding fluidic actuators by pressurizing cavities within the body. In this paper, we present a novel approach to soft robot fabrication using soft expanding foam as the base material. While recent research points to elastic foams as a means to reduce material, manufacturing costs, and robot mass, they have not been explored much in the literature. This paper presents fabrication and prototyping techniques for developing low cost, custom-shaped soft robots from expanding polyurethane foam. We describe how to integrate user-defined routing points for transmission and actuation through cable-driven electrical actuation systems directly into the foam. Furthermore, we explore novel fabrication and prototyping techniques in order to build and integrate soft sensors into the foam substrate, which we demonstrate on soft robots varying in design complexity from a soft gripper to a soft "puppy".**

***Index Terms*—Soft Robot Applications, Soft Robot Materials and Design, Soft Sensors and Actuators, Tendon/Wire Mechanism**

I. Introduction

THE defining feature of soft robotics systems is that they consist predominantly of materials similar to human tissue in terms of elastic moduli [1], [2]. The main components of these systems are the *soft robot structure* itself [3], [4], alongside *sensing*, *transmission*, and *actuation* components. All four components need to be made of, or built into, a soft base material, imposing constraints on the choice of materials and fabrication methods. Recent advances in soft robotics research have enabled the use of new soft materials by developing novel fabrication and prototyping techniques, each tailored to a particular material [5], [6], [7]. Previously studied materials include silicone elastomers, urethanes, hydrogels [8], [9], braided fabrics, hydraulic fluids, liquid metal conductors, and many more. For instance, silicone elastomers are often used for the soft robot structure. Their non-porosity favours fluidic transmission and actuation [10], [11], as well as sensing based on micro-channels containing liquid metal conductors [12], [13] such as EGaIn (Eutectic Gallium Indium).

In this paper, we focus on robots made of soft elastic foam. While both the micro- and macro-scale mechanical behaviour of these foams has been studied experimentally and numerically in various works [14], [15], [16], such expanding foams have not been studied extensively for soft robotics applications. Poroelastic foams encapsulated in a PDMS (polydimethylsiloxane), or in a silicone elastomer sealing layer, have been used for fabricating soft fluidic actuators [17], [18], [19]. Previous work also investigated tendon-based actuation and transmission systems [20], [21], [22]. In [20], [22], tendons were sewed through a fabric "skin" placed around the soft robot in order to reduce friction. Both of these previous tendon and fluidic transmission approaches not only add an extra step to the fabrication process of the soft robot, but also introduce associated uncertainties and failure risks.

Some prior work on embedded soft sensors in foam structures include deformation sensing [23] and tactile contact detection [24]. The former [23] relies on robotic fabrics attached to the surface of the foam, where the motion of the fabric relative to the foam surface may add noise or drift to the signal. Furthermore, this approach adds considerable bulk around the soft structure. The latter [24] embeds infrared LEDs and phototransistors into soft urethane foam to provide multi-axis tactile information. They manually embed discrete traditional electronics components in a grid like pattern, making the fabrication process cumbersome with increasing area. To the best of our knowledge, a compatible sensing technique for deformations of custom-shaped foam-bodied soft robots is not available in prior work.

In this paper, we present the following contributions:

- Novel fabrication and prototyping techniques for fabricating foam-bodied soft robots, which integrate compatible *soft sensing, transmission, and actuation*;
- An improved transmission system for foam-bodied tendon-driven soft robots, which is incorporated while fabricating the soft robot structure itself, thus *avoiding any additional "skin" or extra fabrication steps*;

Manuscript received: September, 10, 2018; Revised December, 20, 2018; Accepted January, 1, 2019.

This paper was recommended for publication by Editor Cho, Kyu-Jin upon evaluation of the Associate Editor and Reviewers' comments.

This work was partially funded by the ETH Zürich Postdoctoral Fellowship no. 18-1 FEL-09.

Luca Somm, David Hahn, Nitish Kumar and Stelian Coros are with the Computational Robotics Lab at the Institute for Pervasive Computing, ETH Zurich, Zurich 8092, Switzerland. {somml@student.ethz.ch, david.hahn@inf.ethz.ch, nitish.kumar@inf.ethz.ch, stelian.coros@inf.ethz.ch}

Digital Object Identifier (DOI): see top of this page.

*corresponding author

- Fabrication and prototyping techniques for novel soft sensors, which can be manufactured either as stand-alone devices, or more importantly, integrated into our foam-bodied soft robot structures.
- We also demonstrate the flexibility of our approach by manufacturing some custom-shaped foam robots of varying complexity from a soft gripper to a soft "puppy", and
- Experimentally assess our sensing and actuation methods in a tele-manipulation master-slave setup.

The rest of this paper is organized as follows: in section II we first discuss expanding foam as the base material for our soft robot structures. We also elaborate on our fabrication and prototyping techniques for our embedded tendon-driven actuation system. In section III, we then focus on our soft sensors, describing fabrication and prototyping techniques, as well as their integration into the soft robot structure. We then present our experimental results, in particular the demonstrators we have manufactured, in section IV. We conclude our discussion in section V, addressing specific challenges in the current work and possible directions for future work.

II. Soft Robot Structure Fabrication

In this section, we first describe the materials we use to fabricate our soft robots, as well as some general design concepts that follow from the material properties. The main motivation for the choices we make here is that these robots should be low-cost and could be fabricated without the need for specialised hardware or expert knowledge. We then describe the design and fabrication process in detail and finally demonstrate the effectiveness of our approach on some prototypes.

A. Materials

We choose soft polyurethane (PU) foam as the base material for our soft robots. In particular, we use "FlexFoam-iT!™" types III and V from SmoothOn Inc. for our experiments, see [25] for details. These foams are two-component expanding foams that remain soft after curing. They can be mixed manually and cure within a few hours at room temperature, allowing for fast and cost-effective prototyping of our soft robots.

Predicting the exact volume expansion ratio of these foams can be difficult [26], as it may depend on various factors such as the relative amount of each component added to the mixture, ambient temperature, as well as the mould geometry. In our experiments we observed some deviations from the manufacturer specifications; overall, however, we were able to produce reasonably consistent results in terms of foam expansion ratio and bulk mechanical properties, see Table I. If a small amount of foam overflows the mould during the expansion process, we simply cut it away once the foam is fully cured.

Another important feature of these PU foams is that they easily bond to many other materials as they cure. While this behaviour requires the application of a wax-based release agent (Ease Release™ 2831, [25]) in order to remove the cured foam from its mould, it also allows us to directly incorporate small 3D printed *tendon routing pins* into the foam, see Fig. 1. Our soft robots can then be actuated by threading strings through these pins and connecting each tendon to an off-the-shelf servo motor. We route the tendons along the surface of our robots and space the routing pins close enough to one another along each tendon, such as to keep the tendons from touching the foam during most deformations. In order to preserve a smooth surface, we recede the tendons into small grooves along the robot's surface. This way we achieve good actuation behaviour with low friction loss, while ensuring that tendons or routing pins rarely come into contact with any other objects our soft robots might interact with. We also avoid the need for placing an additional "skin" on top of the foam, which would complicate the manufacturing process.

We build free-form moulds for our soft robots from acrylonitrile styrene acrylate (ASA), [27], using a Stratasys F370 3D printer [28]. The layer height (printing resolution) is approximately $1/4$ mm. We use the same material to 3D print the tendon routing pins and common string as tendons. We

FlexFoam-iT!™	type III	type V
Mix ratio (A:B by mass)	57.5:100	105:100
Expected foam density [g/l]	48	80
A+B by mass per expanded volume [g/l]	28+49	81+77
Experimental foam density [g/l]	75 $\pm$ 10	115 $\pm$ 10

TABLE I: Foam material properties: Mix ratio by mass and expected foam density as per manufacturer datasheet [25]; mixing mass determined experimentally (input mass of components A and B per resulting expanded foam volume); experimentally observed foam density (exceeds manufacturer specification). Some of the foaming agent dissipates during the expansion. We believe that the higher foam density observed in our experiments is to some extent due to the internal pressure building up inside of the mould, as we aim to err on the side of caution, i. e. over- rather than under-filling the mould.

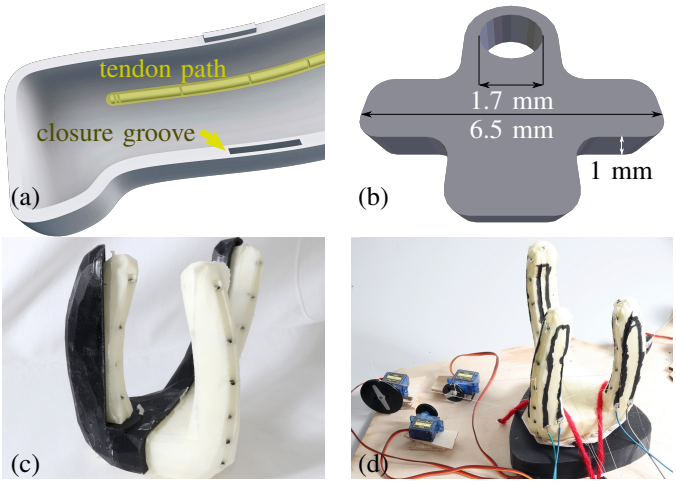

Fig. 1: Mould design showing tendon path with cylindrical inset and gaps where pins are held in place, as well as mould closure aids (a); pin geometry (b); fabricated part with pins in place (c); actuated soft gripper (d).

have observed excellent bonding between the PU foam and the ASA pins, allowing for a remarkably small pin geometry as shown in Fig. 1b.

B. Fabrication

We start the fabrication process by designing the geometry of the soft robot we intend to build. We use free-form smooth surface modelling based on Catmull-Clark subdivision surfaces [29] available in the open-source software Blender [30]. Once the general shape of the robot is defined, we choose paths along its surface where we wish to place tendons for actuation. Typically, we aim for 3 tendons at approximately $120°$ angles for omni-directional bending of cylinder-like structures, such as fingers or legs. For simpler examples, basic unidirectional bending can be achieved with a single tendon, as the foam's elastic behaviour is sufficient to return the material to its rest shape without the need for an antagonistic tendon.

We prevent the tendon routing pins from protuding out of the robot's surface by cutting out grooves of 2 mm radius along the tendon path. We leave gaps of the same size as the pin thickness, spaced at roughly 5 cm intervals along these grooves. After the mould has been printed, we can push the tendon routing pins into these gaps to hold them in place while the expanding foam flows around and bonds to them as it cures. We occasionally choose a denser spacing in highly curved regions. The Boolean difference of the robot model minus the groove shapes defines the inside surface of the mould; Figs. 1a and 2 show examples of these tendon grooves with pin placement gaps.

The mould modelling concludes by computing the Boolean difference of an inflated (or "fattened") copy of the model (encasing the entire model) minus the designed shape. We also remove excess volume to reduce 3D printing time and material costs, generally aiming for 5 mm thick walls throughout the mould. Of course, we want to be able to re-use our moulds for creating multiple copies of each robot. Consequently, we split the mould model into multiple pieces, such that the foam can be removed easily after disassembling the mould. Note that due to the flexibility of the foam, the pieces of the mould can have some concave regions without interfering with the removal process. In order to facilitate properly aligning all the pieces and closing the mould quickly after adding the expanding foam, we also add tongue-and-groove structures along the edges of the pieces in the modelling phase.

We use Blender [30] for the entire modelling pipeline from shape design to printable mould pieces. While we perform these tasks manually for all of the prototypes presented in this paper, Blender does offer a powerful scripting interface such that this process can be automated in future work. At this point we are ready to send the virtual models of all the individual mould pieces to the 3D printer. Once all the pieces are printed and cleaned, we can now manufacture the actual soft robot. We first apply the release agent, and place tendon routing pins into the prepared gaps. We then fill and close the mould, rotating it slowly to allow the foam to flow around and enclose all the pins. When the foam has cured (after about one hour), we remove the robot from the mould and thread the tendons through the pins. Because the foam bonds directly to the pins, we do not require any additional glue to hold them in place. Even our small pin geometry (Fig. 1b) can withstand forces up to 15 N in the normal direction and 20 N in the tangential direction (along the tendon). In fact, tearing the pins out of the foam actually tears the foam in the vicinity of the pin, but does not lead to debonding.

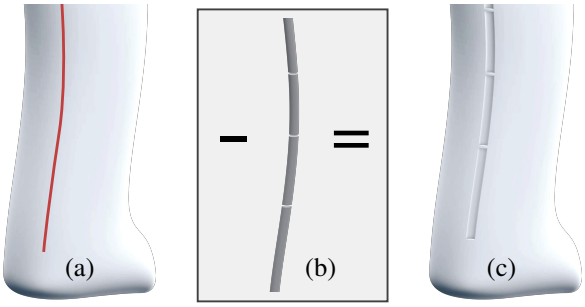

Fig. 2: Given some initial shape for our soft robot with a desired tendon path (a), we first extrude a circular cross section along the path and leave gaps where pins will be placed (b); we then use the result to cut the initial shape, leaving a groove for the tendon (c). The shape shown in image (c) then becomes the inside surface of the 3D printed mould.

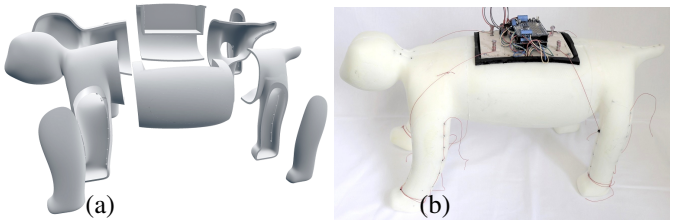

Fig. 3: Our four-legged soft robot: (a) designed mould pieces and (b) final result.

The soft robotic gripper (Fig. 1c & d) is our first "organic" free-form design that was implemented and fabricated using the techniques presented in this paper. It has 3 fingers, with three tendons each for actuation. We also built a fairly large four-legged foam creature (the "soft puppy"), see Fig. 3, again embedding routing pins for 3 tendons per leg, such that two tendons can support a forward walking motion, while the third can bring the leg forward for the next walking cycle. We also leave some space in its belly where we can install actuators. This example shows that our foam-moulding technique allows us to manufacture large, arbitrary-shaped soft robots in a single moulding step, and that the inclusion of tendon routing pins also works well for these larger moulds. We use type-V foam [25] for both of these examples.

III. Soft Sensor Fabrication and Integration

While PU foam itself is an insulator, conductive varieties are available off-the-shelf, such as those used in commercial packaging of industrial electronics. However, these conductive foams usually have very low volume conductivity and come in pre-defined simple shapes such as thin sheets. Consequently, there is no possibility to modify the conductive properties, and

(a) soaked (b) coated (c) channel

Fig. 4: Different sensor fabrication techniques and cylindrical test specimens for compressive loading experiments.

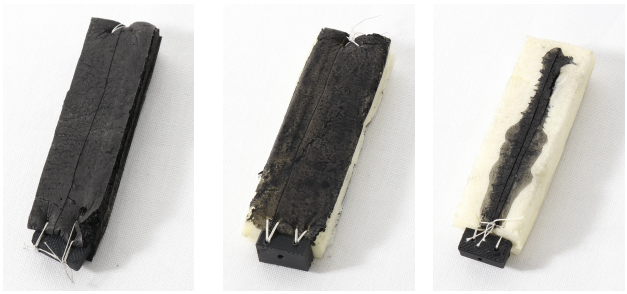

(a) soaked (b) coated (c) channel

Fig. 5: Different sensor fabrication techniques and rectangular test specimens for tensile loading experiments.

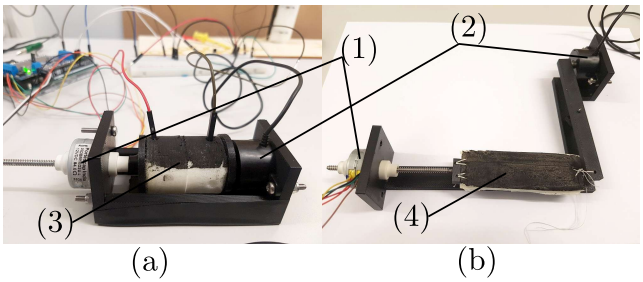

Fig. 6: Experimental setup used for (a) compression loading and (b) tensile loading experiments. The components used in the setup are (1) stepper motor, (2) force sensor, (3) & (4) soft sensors.

little room for customizing the shape of soft sensors based on pre-manufactured foam. This section describes how we fabricate our soft sensors and embed them into our foam-bodied soft robots. The techniques described in section II enable us to fabricate such custom-shaped soft structures. In this section, we now investigate how to introduce soft sensing into our soft robot fabrication process.

A. Fabrication techniques

The driving idea behind our soft sensors is to modify the conductivity of the PU foam in a localized and task-specific way to enable sensing of the foam's own deformation. In order to achieve the desired conductivity in the foam substrate, we prepare a conductive "ink", binding carbon powder of $50\,\mathrm{nm}$ particle size (Vulcan XC72r) with regular acrylic colour (Caran D'Ache) and mixing the resulting conductive paint with water and a commodity emulsifying agent. We add 3 units of carbon powder, 2.5 units of acrylic colour, and 6 units of emulsifying agent per 100 units of water by weight. Also note that using carbon or metal powder of larger particle size, as well as mixing the powder directly into the foam, did not produce the desired results in our experiments.

We present three different sensor fabrication techniques based on this conductive ink. In the first approach, we *soak* the whole soft substrate in the conductive ink, as shown in Figs. 4a and 5a. The second method is to *coat* the surface of the soft substrate with conductive ink, as shown in Figs. 4b and 5b. Finally, the third technique is to form a *channel* in the foam by making a shallow cut in the soft substrate and depositing a small quantity of conductive ink into it with a syringe, as shown in Figs. 4c and 5c. We perform compression tests on the cylindrical samples, Figs. 4 and 6a, and tension tests on the rectangular specimens, Figs. 5 and 6b. The cylindrical soft sensors have a radius of approximately 10 mm and are 60 mm long (except the soaked specimen, which is only 23 mm long). The rectangular soft sensors' dimensions are ca. $10 \times 20 \times 100$ mm. The next section covers the results of these experiments.

B. Experimental results

The experimental setup for our tensile and compressive loading tests, as shown in Fig 6, is as follows: a micro-controller (Arduino Mega 2560) drives a stepper motor (1), (Portescap, 26DBM10D2U-L) deforming the soft sensor (3), (4), and also logs the resulting forces at an additional sensor (2), (TE Connectivity Measurement Specialties FC2231-0000-0010-L), as well as the resistance of the soft sensor using a voltage divider circuit. The resulting data is sent to a PC over the serial bus and recorded with the help of *Gobetwino*. Figures 7 and 8 show the results of compressive tests on the cylindrical soft sensors (Fig. 4) and tensile tests on the rectangular soft sensors (Fig. 5), respectively. For both compressive and tensile tests, we report force and resistance values in 1 mm increments of deformation. We show multiple loading and unloading cycles of each soft sensor specimen and for each experiment in Figs. 7 and 8.

During the compression experiments, the test specimens were deformed by up to 10 mm. In general, we observe a non-linear transfer function from displacement to resistance and also a lot of noise in the signal. The soaked cylinder (Fig. 7a) shows the best signal-to-noise characteristics, indicating that continuous mapping of compressive stress to sensor readout might be possible. For the other two fabrication techniques (Fig. 7b and c), the signal is more pronounced at peak strain levels, making them suitable for detecting certain strain thresholds only. During the tensile experiments, the test specimens were deformed by up to 15 mm. Again, the transfer function from displacement to resistance is non-linear, but shows a much more continuous response compared to the compression tests. The signal to noise ratio is also a lot better under tension, especially for the channel fabrication technique (Fig. 8c). For the soaked and surface coated soft sensors (Fig. 8a and b), we observe significant signal attenuation in subsequent loading cycles.

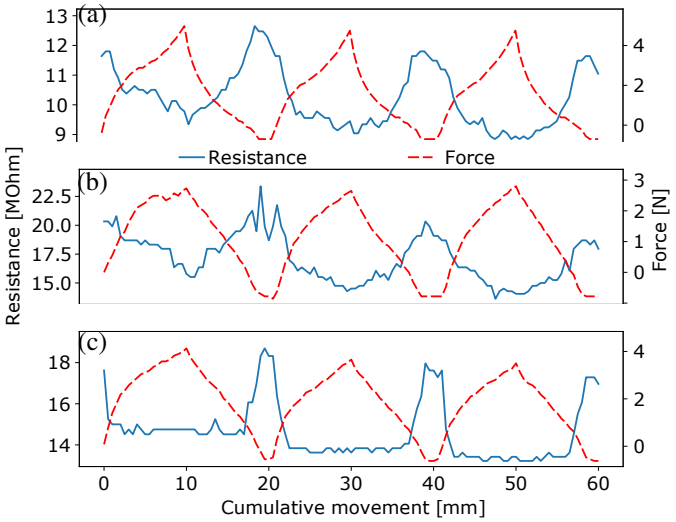

Fig. 7: Compression loading results for soft sensors with (a) soaked (b) surface painted and (c) embedded channels.

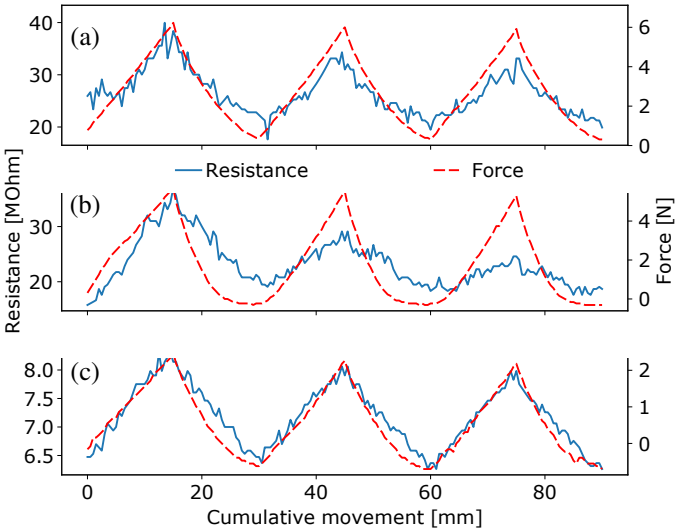

Fig. 8: Tensile loading results for soft sensors with (a) soaked (b) surface painted and (c) embedded channels.

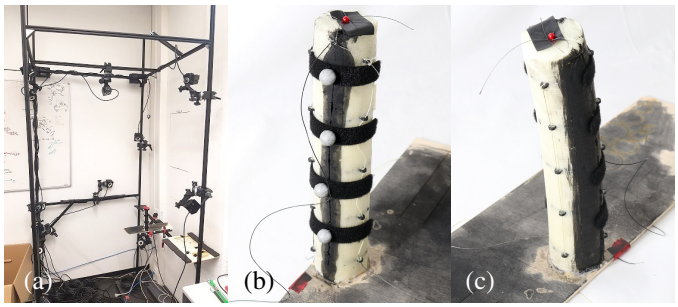

Fig. 9: Bending experiment with a cylindrical actuator embedded with conductive type channel sensors (a) Optitrack motion capture system (b) cylindrical actuator showing the tendon routing and (c) embedded conductive channel on the opposite side of the tendon.

In summary, our soft sensors generally perform better for tensile rather than for compressive strain. The unsatisfactory behaviour under compression is likely due to buckling of the surface. With respect to embedding these sensors into larger soft robots, manufactured as a single piece of foam, clearly surface coating and conductive channels can be added a lot easier than soaking parts of the robot in conductive ink. Creating soaked soft sensors has the additional drawbacks of requiring more conductive ink and being a more laborious process compared to the other two fabrication methods. Furthermore, when making the whole volume conductive, many deformations may result in the same overall resistance when some parts of the body stretch while others compress; we expect this effect to be even more pronounced for larger soft sensors. Consequently, soaked soft sensors would be more effective as small strain sensors for measuring localized deformations. Our surface coating or channel fabrication techniques yield more freedom with respect to how these sensors are embedded in the soft robot body. Furthermore, in particular our channel-type sensors show very promising characteristics in tensile strain tests, including approximately linear response, as well as low signal loss on subsequent cycles. Consequently, we focus on our channel fabrication technique in the following discussion on soft sensing and embedded sensors for soft robots.

Actuating a soft robot via tendons typically leads to smooth bending deformations. In terms of embedded sensing, we therefore test such a tendon actuated bending structure first. Our test specimen is a cylinder of 20 mm radius and 200 mm height, with a tendon routed through five pins (Fig. 9b). We embed a conductive channel on the side opposite of the tendon as a deformation sensor (Fig. 9c). We then bend the cylinder by manually pulling on the tendon. Due to possible local buckling of the concavely deformed part of the surface, the deformation of this bending cylinder cannot be easily calculated from the distance the tendon is pulled. Consequently, we equip the cylinder with four optical markers placed on top of the conductive channel, and track these markers with a motion capture system consisting of 10 *OptiTrack Prime 13* cameras. The resulting data allows us to measure the distances between the markers and thus approximate the elongation of the surface in the vicinity of the embedded sensor. In Fig. 10, we show that the change in resistance values of the conductive channel correlates very nicely with the approximated arc length on the surface. Please also note that the sensor is able to capture fast dynamics of the bending motion as demonstrated by the stair-stepped shape of the input deformation during the second and third deformation cycle (Fig. 10, $t \approx 8 \ldots 16$ s). We re-tested the same bending sensor after a period of ca. 8 months to quantify the effect of ageing on the signal-to-noise ratio (SNR). The SNR dropped only slightly from 10.92 dB to 9.60 dB, as shown in Fig. 11.

IV. Application Demonstrators

Having established these fabrication methods for both our custom-shaped soft robots, as well as for our soft deformation sensors in the previous sections, we now demonstrate how to integrate these soft structure and sensor fabrication techniques

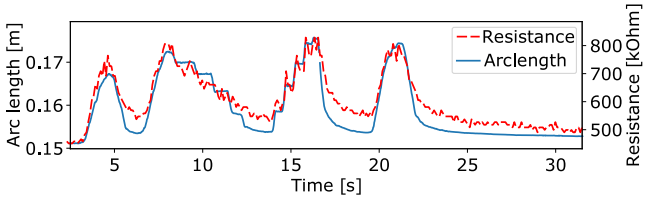

Fig. 10: Results from the bending experiment.

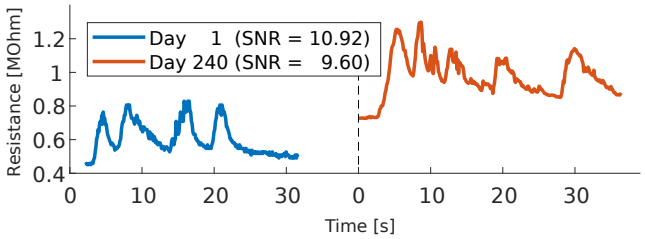

Fig. 11: Sensor ageing; left: original data from Fig. 10; right: repeat of the experiment on the same sensor as in Fig. 9 ca. 8 months later.

in order to manufacture custom-shaped soft robots capable of sensing their own deformation.

A. *Soft robotic hand*

Figure 12a shows a soft robotic hand with two servo actuators, one for controlling the thumb and another for the four fingers together. We measure the movements of the thumb and the middle finger using a soft wearable device with two channel-type sensors as shown in Fig. 12b. We then map the measured motion to the soft robotic hand via a linear transformation. Both master and slave device are fabricated from the exact same mould. We perform dynamic movements with the soft wearable device, which are then reproduced by the slave soft robotic hand. The correlation between the mapped actuation of the servos and the measured resistance is shown in Fig. 13. The resistance measured via embedded soft sensing in the wearable device shows the range of the user's dynamic movements we are able to capture (please also refer to the accompanying video).

B. *Soft robotic gripper*

The soft robotic gripper (Fig. 1c), uses three tendons per finger such that one tendon opens the grip, while the other

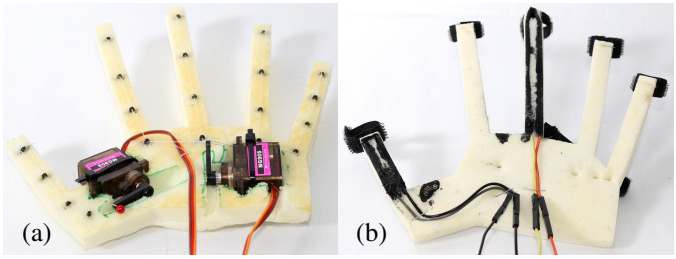

Fig. 12: Actuated soft hand as slave device (a) and passive soft wearable with embedded sensing as master device (b).

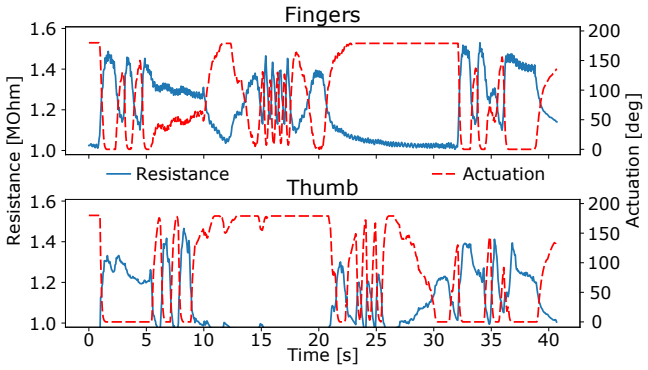

Fig. 13: Thumb and middle finger movements as measured by the embedded conductive channel-type soft sensor.

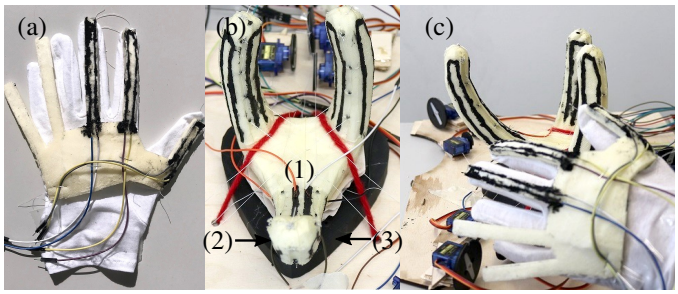

Fig. 14: Soft glove (a), soft gripper (b) with embedded channel-type sensors (1, 2, 3); full experimental master-slave set-up (c).

two tighten the grip and adjust the position of the finger. Each finger has three embedded channel-type sensors, as shown in Fig. 14b. We use a new soft wearable glove with the same geometry as in Fig. 12b for the foam part. This foam part contains three channel-type sensors and is sewed onto the

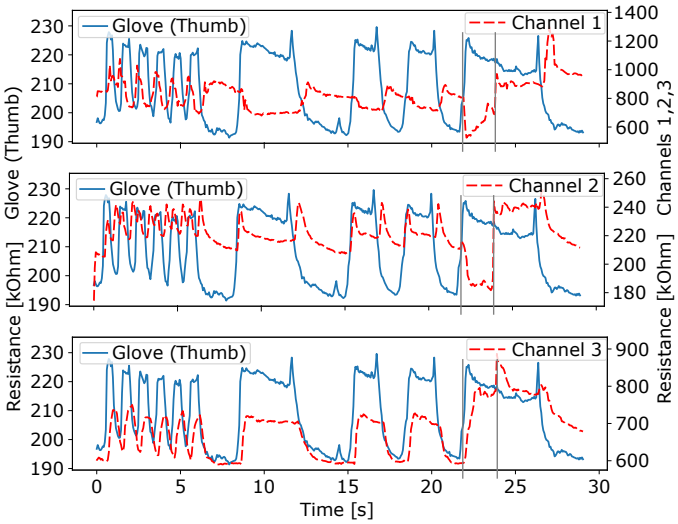

Fig. 15: Resistance values from the three channel-type sensors embedded in the robotic gripper. The gripper is obstructed from $t \approx 22$ s to $t \approx 24$ s, indicated by the vertical bars. Please also refer to our accompanying video.

fabric of a glove. We use this glove as the master device to actuate our gripper. The thumb on the glove controls the longer finger on the gripper. Figure 15 shows the sensor reading from the glove's thumb alongside the three readings from the actuated finger (Fig. 14b & c). We move only the thumb in this experiment, showing the relationship between the user's hand motion (mapped from the sensor on the glove) and the measured deformation values from the sensors on the gripper. We show six rapid thumb movements, followed by three slower motion cycles. The movement of the gripper's finger is obstructed from $t \approx 22$ s to $t \approx 24$ s. Please note how sensor readings from the gripper follow the sensor reading from the glove when the actuated gripper is not obstructed, but deviate substantially when the gripper cannot move freely. Please refer to the accompanying video for a full tele-manipulation demonstration, where user hand motion from all three fingers controls the entire robotic gripper.

V. Discussion, conclusion and future work

In this paper, we have explored various possibilities for using expanding PU foam as a new soft material for building custom-shaped, low-cost soft robots in detail. All the four aspects of soft robot functionality, namely fabrication, actuation, transmission, and sensing, have been discussed. By fabricating user-defined shapes, such as the soft gripper and the soft puppy, we have demonstrated the versatility of the presented methods and tools. Choosing tendon-driven actuation and integrating user-defined routing points for transmission during the fabrication process itself enables us to streamline the fabrication process, which we hope will allow non-expert users to design and deploy their own soft robots more effectively. We also presented different soft sensor fabrication techniques, allowing the user to fabricate different types of soft sensors and to customize the soft sensor integration into the soft robot structure according to functional requirements, in particular to sense specific deformations. This kind of complete integration of transmission, actuation, and sensing functionality into the soft robot body will allow for much more interactive soft robots that can respond to external stimuli. We believe that our approach leads to a range of possible new routes for finding and establishing an effective way of sensing in soft robots.

The soft robot structure fabrication techniques presented in this paper are quite scalable as the soft robot body grows in size. Nevertheless, at some point the moulds will need to be split into several parts due to 3D printing restrictions, and the foam pouring process becomes more challenging. So far, our tools and methods were implemented manually, however, some steps (such as the mould design) have great potential for automation. In future work, we aim to build an automated setup for generating printable mould pieces from a given user-defined surface shape, which is not trivial for organic shapes like the soft gripper and soft puppy presented in this paper. Similarly, we might also allow for a more interactive placement of tendon routing points or provide a set of suggestions from which the user can choose a preferred tendon layout for transmission. Numerical simulation tools, such as finite element methods, can be used to describe the micro and macroscopic deformation behaviour of foam-bodied soft robots [31], [32]. We plan to use such simulations in future work to inform and improve our soft robot design process.

Our soft sensors, especially channel-type sensors, can be used for quantitative analysis, deformation, or pose estimation. However, there are certain issues such as decreasing sensor signals over cyclic loading scenarios, in particular with soaked and surface-coated sensors, as well as time-dependent drift of the signal due to the inherently viscoelastic nature of the PU foam material. In future work, we aim to take this viscoelasticity into account and compensate for these effects, which would make the soaked or coated soft sensor readings more robust. There is a slight effect on the signal-to-noise due to ageing of the sensors when tested over an extended time-span. However, there are a number of factors apart from ageing that could also affect the SNR, such as the electrical contact between the readout wires and the soft sensor. Over time, the conductive ink might also become drier leading to an increased baseline resistance of the sensor. As our sensor fabrication method is simple, sensors can be "refreshed" quite easily by adding more conductive ink later on. Currently, our soft sensors are fabricated manually, leading to inconsistencies in the depth of the cut, or the amount of the conductive ink deposited. In future work, we aim to improve the precision and build a special tool for "tattooing" channel-type sensors into the foam in a more consistent way.

VI. Acknowledgment

We are thankful to Pol Banzet for his help with fabricating and testing of the X-walker soft robot shown in the video.

References

[1] C. Lee, M. Kim, Y. J. Kim, N. Hong, S. Ryu, H. J. Kim, and S. Kim, "Soft robot review," *International Journal of Control, Automation and Systems*, vol. 15, no. 1, pp. 3–15, Feb. 2017. [Online]. Available: https://link.springer.com/article/10.1007/s12555-016-0462-3

[2] S. Coyle, C. Majidi, P. LeDuc, and K. J. Hsia, "Bio-inspired soft robotics: Material selection, actuation, and design," *Extreme Mechanics Letters*, vol. 22, pp. 51–59, July 2018. [Online]. Available: http://www.sciencedirect.com/science/article/pii/S2352431617302316

[3] K.-J. Cho, J.-S. Koh, S. Kim, W.-S. Chu, Y. Hong, and S.-H. Ahn, "Review of manufacturing processes for soft biomimetic robots," *International Journal of Precision Engineering and Manufacturing*, vol. 10, no. 3, pp. 171–181, July 2009. [Online]. Available: https://doi.org/10.1007/s12541-009-0064-6

[4] F. Schmitt, O. Piccin, L. Barbé, and B. Bayle, "Soft Robots Manufacturing: A Review," *Frontiers in Robotics and AI*, vol. 5, 2018. [Online]. Available: https://www.frontiersin.org/articles/10.3389/frobt.2018.00084/full

[5] C. Laschi and M. Cianchetti, "Soft Robotics: New Perspectives for Robot Bodyware and Control," *Frontiers in Bioengineering and Biotechnology*, vol. 2, 2014. [Online]. Available: https://www.frontiersin.org/articles/10.3389/fbioe.2014.00003/full

[6] C. Laschi, "Soft Robotics Research, Challenges, and Innovation Potential, Through Showcases," in *Soft Robotics*. Springer, Berlin, Heidelberg, 2015, pp. 255–264. [Online]. Available: https://link.springer.com/chapter/10.1007/978-3-662-44506-8_21

[7] C. Laschi, B. Mazzolai, and M. Cianchetti, "Soft robotics: Technologies and systems pushing the boundaries of robot abilities," *Science Robotics*, vol. 1, no. 1, Dec. 2016. [Online]. Available: http://robotics.sciencemag.org/content/1/1/eaah3690

[8] J.-Y. Sun, X. Zhao, W. R. K. Illeperuma, O. Chaudhuri, K. H. Oh, D. J. Mooney, J. J. Vlassak, and Z. Suo, "Highly stretchable and tough hydrogels," *Nature*, vol. 489, no. 7414, pp. 133–136, Sept. 2012. [Online]. Available: https://www.nature.com/articles/nature11409

[9] H. Yuk, S. Lin, C. Ma, M. Takaffoli, N. X. Fang, and X. Zhao, "Hydraulic hydrogel actuators and robots optically and sonically camouflaged in water," *Nature Communications*, vol. 8, 02 2017.
[10] B. Mosadegh, P. Polygerinos, C. Keplinger, S. Wennstedt, R. F. Shepherd, U. Gupta, J. Shim, K. Bertoldi, C. J. Walsh, and G. M. Whitesides, "Pneumatic Networks for Soft Robotics that Actuate Rapidly," *Advanced Functional Materials*, vol. 24, no. 15, pp. 2163–2170, Apr. 2014. [Online]. Available: https://onlinelibrary.wiley.com/doi/abs/10.1002/adfm.201303288
[11] A. Zatopa, S. Walker, and Y. Menguc, "Fully Soft 3d-Printed Electroactive Fluidic Valve for Soft Hydraulic Robots," *Soft Robotics*, vol. 5, no. 3, pp. 258–271, June 2018.
[12] Y.-L. Park, C. Majidi, R. Kramer, P. Bérard, and R. J. Wood, "Hyperelastic pressure sensing with a liquid-embedded elastomer," *Journal of Micromechanics and Microengineering*, vol. 20, no. 12, 2010. [Online]. Available: http://stacks.iop.org/0960-1317/20/i=12/a=125029
[13] Y.-L. Park, B. rong Chen, and R. J. Wood, "Design and fabrication of soft artificial skin using embedded microchannels and liquid conductors," *IEEE Sensors Journal*, vol. 12, no. 8, pp. 2711–2718, August 2012.
[14] D. Weaire and M. A. Fortes, "Stress and strain in liquid and solid foams," *Advances in Physics*, vol. 43, no. 6, pp. 685–738, dec 1994.
[15] D. Weaire and S. Hutzler, *The physics of foams*. Clarendon Press, 1999.
[16] W.-Y. Jang, A. M. Kraynik, and S. Kyriakides, "On the microstructure of open-cell foams and its effect on elastic properties," *International Journal of Solids and Structures*, vol. 45, no. 7-8, pp. 1845–1875, april 2008.
[17] B. C. M. Murray, X. An, S. S. Robinson, I. M. v. Meerbeek, K. W. O'Brien, H. Zhao, and R. F. Shepherd, "Poroelastic Foams for Simple Fabrication of Complex Soft Robots," *Advanced Materials*, vol. 27, no. 41, pp. 6334–6340, Nov. 2015. [Online]. Available: https://onlinelibrary.wiley.com/doi/abs/10.1002/adma.201503464
[18] M. A. Robertson and J. Paik, "New soft robots really suck: Vacuum-powered systems empower diverse capabilities," *Science Robotics*, vol. 2, no. 9, Aug. 2017. [Online]. Available: http://robotics.sciencemag.org/content/2/9/eaan6357
[19] C. C. Futran, S. Ceron, B. C. M. Murray, R. F. Shepherd, and K. H. Petersen, "Leveraging fluid resistance in soft robots," in *2018 IEEE International Conference on Soft Robotics (RoboSoft)*, Apr. 2018, pp. 473–478.
[20] J. M. Bern, G. Kumagai, and S. Coros, "Fabrication, modeling, and control of plush robots," in *2017 IEEE/RSJ International Conference on Intelligent Robots and Systems (IROS)*, Sept. 2017, pp. 3739–3746.
[21] C. M. Donatelli, Z. T. Serlin, P. Echols-Jones, A. E. Scibelli, A. Cohen, J. Musca, S. Rozen-Levy, D. Buckingham, R. White, and B. A. Trimmer, "Soft foam robot with caterpillar-inspired gait regimes for terrestrial locomotion," in *2017 IEEE/RSJ International Conference on Intelligent Robots and Systems (IROS)*, Sept. 2017, pp. 476–481.
[22] J. P. King, D. Bauer, C. Schlagenhauf, K.-H. Chang, D. Moro, N. Pollard, and S. Coros, "Design , Fabrication , and Evaluation of Tendon-Driven Multi-Fingered Foam Hands," in *IEEE-RAS International Conference on Humanoid Robotics (Humanoids)*, 2018.
[23] J. C. Case, J. Booth, D. S. Shah, M. C. Yuen, and R. Kramer-Bottiglio, "State and stiffness estimation using robotic fabrics," in *2018 IEEE International Conference on Soft Robotics (RoboSoft)*, Apr. 2018, pp. 522–527.
[24] A. Kadowaki, T. Yoshikai, M. Hayashi, and M. Inaba, "Development of soft sensor exterior embedded with multi-axis deformable tactile sensor system," in *RO-MAN 2009 - The 18th IEEE International Symposium on Robot and Human Interactive Communication*, Sept. 2009, pp. 1093–1098.
[25] Smooth-On, Inc. (2018) FlexFoam-iT!™ Series, Technical Overview. [Online]. Available: http://www.smooth-on.com/tb/files/FLEXFOAM-IT_SERIES.pdf
[26] M. T. Tolley, R. F. Shepherd, B. Mosadegh, K. C. Galloway, M. Wehner, M. Karpelson, R. J. Wood, and G. M. Whitesides, "A Resilient, Untethered Soft Robot," *Soft Robotics*, vol. 1, no. 3, pp. 213–223, Sept. 2014. [Online]. Available: https://doi.org/10.1089/soro.2014.0008
[27] Stratasys, Ltd. (2018) ASA Material Datasheet. [Online]. Available: http://www.stratasys.com/-/media/files/material-spec-sheets/mss_fdm_asa_0418a.pdf
[28] ——. (2018) The Stratasys F123 Series. [Online]. Available: http://www.stratasys.com/-/media/files/printer-spec-sheets/pss_fdm_f123series_1017a.pdf
[29] E. Catmull and J. Clark, "Recursively generated B-spline surfaces on arbitrary topological meshes," *Computer-Aided Design*, vol. 10, no. 6, pp. 350 – 355, 1978. [Online]. Available: http://www.sciencedirect.com/science/article/pii/0010448578901100
[30] Blender, v2.79b. [Online]. Available: https://www.blender.org/
[31] J. M. Bern, K.-H. Chang, and S. Coros, "Interactive Design of Animated Plushies," *ACM Trans. Graph.*, vol. 36, no. 4, pp. 80:1–80:11, July 2017. [Online]. Available: http://doi.acm.org/10.1145/3072959.3073700
[32] C. Schlagenhauf, D. Bauer, K.-H. Chang, J. P. King, D. Moro, S. Coros, and N. Pollard, "Control of Tendon-Driven Soft Foam Robot Hands," in *IEEE-RAS International Conference on Humanoid Robotics (Humanoids)*, 2018.